AD-A051 139 CALIFORNIA UNIV LOS ANGELES DEPT OF MATERIALS F/G 11/6
ANISOTROPIC ACOUSTIC EMISSION BEHAVIOR OF HSLA STEELS.(U)
JAN 78 K ONO, G HUANG, A KAWAMOTO N00014-75-C-0419
UNCLASSIFIED TR-78-01 NL

| OF |
AD
A051139

END
DATE
FILMED
4-78
DDC

(12)

Technical Report No. 78-01

to the

Office of Naval Research

Contract No. N00014-75-C-0419

ANISOTROPIC ACOUSTIC EMISSION BEHAVIOR OF HSLA STEELS

K. Ono, G. Huang* and A. Kawamoto**
Materials Department
School of Engineering and Applied Science
University of California
Los Angeles, California 90024

*Effect Technology Inc., Santa Barbara, California
**Sharp Electric Co., Osaka, Japan

January 1978

SECURITY CLASSIFICATION OF THIS PAGE *(When Data Entered)*

REPORT DOCUMENTATION PAGE

READ INSTRUCTIONS BEFORE COMPLETING FORM

1. REPORT NUMBER ~~78-02~~ (14) TR-78-01
2. GOVT ACCESSION NO.
3. RECIPIENT'S CATALOG NUMBER

4. TITLE *(and Subtitle)* (6) Anisotropic Acoustic Emission Behavior of HSLA Steels •
5. TYPE OF REPORT & PERIOD COVERED (9) Technical rept.,
6. PERFORMING ORG. REPORT NUMBER

7. AUTHOR(s) (10) Kanji/Ono, G./Huang [redacted] A./Kawamoto
8. CONTRACT OR GRANT NUMBER(s) (15) N[redacted]14-75-C-[redacted]419✓

9. PERFORMING ORGANIZATION NAME AND ADDRESS
University of California, Los Angeles, CA 90024
10. PROGRAM ELEMENT, PROJECT, TASK AREA & WORK UNIT NUMBERS

11. CONTROLLING OFFICE NAME AND ADDRESS
Physics Program, Physical Sciences Division
Office of Naval Research, Arlington, VA 22217
12. REPORT DATE (11) Jan[redacted]78
13. NUMBER OF PAGES (12) 19 pp

14. MONITORING AGENCY NAME & ADDRESS *(if different from Controlling Office)*
Office of Naval Research Branch Office
1030 E. Green Street
Pasadena, CA 91101
15. SECURITY CLASS. *(of this report)*
Unclassified
15a. DECLASSIFICATION/DOWNGRADING SCHEDULE

16. DISTRIBUTION STATEMENT *(of this Report)*
Approved for public release, distribution unlimited

17. DISTRIBUTION STATEMENT *(of the abstract entered in Block 20, if different from Report)*

18. SUPPLEMENTARY NOTES
Presented at the 6th International Conference on Internal Friction and Ultrasonic Attenuation in Solids, July 4-7, Tokyo, Japan. To be published in the Proceedings of the conference. Several revisions have been made.

19. KEY WORDS *(Continue on reverse side if necessary and identify by block number)*
Acoutic Emission
Structural Steels
Waveform and Spectrum Analysis
Amplitude Distribution
Non-metallic Inclusions

20. ABSTRACT *(Continue on reverse side if necessary and identify by block number)*
This paper describes acoustic emission behavior of C-Mn steels during tensile tests. Non-metallic inclusions were found to be the primary source of burst-type emission, whereas pearlite shearing was the major origin of continuous-type emission.

DD FORM 1 JAN 73 1473 EDITION OF 1 NOV 65 IS OBSOLETE
S/N 0102-LF-014-6601

SECURITY CLASSIFICATION OF THIS PAGE *(When Data Entered)*

406237

SUMMARY

Wideband acoustic emission (AE) measurements were performed during tensile tests of carbon-manganese steels with different levels of sulphur content. Directionality of AE characteristics was studied via several different AE analysis techniques as well as metallographic observations. Burst-type AE signals observed in the tests of thickness direction samples have been identified as due to MnS inclusions. These signals have quite different frequency spectrum and amplitude distribution characteristics from continuous-type signals during Lüders elongation. The results were correlated to elasticity calculation of the stress field of inclusions.

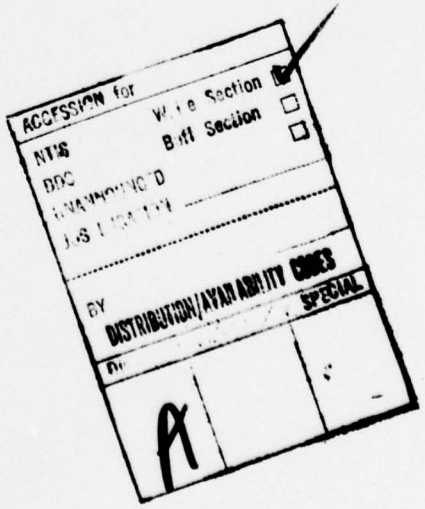

INTRODUCTION

Acoustic emission characteristics of steels have been studied extensively over the last ten years (1-4). Many investigators have attributed distinct AE events or so-called burst emission to one or more of the following processes; a) microyielding or the sudden formation of a slip band, b) the fracture or decohesion of second phase particles, c) microcracking, d) twinning and e) martensitic transformation. Since the confirmation of sources of AE events is generally difficult, few systematic efforts to correlate the results of AE studies to microscopic observation have been made. The continuous AE signals are just as elusive and their origins are yet to be established. Undoubtedly, one source involves the motion of individual dislocations or small groups of dislocations. In this report, results of tensile and AE tests of a C-Mn steel with three different levels of sulphur content are presented and discussed in conjunction with metallographic observations and with elasticity calculations on the stress field of inclusions.

EXPERIMENTAL PROCEDURES

Materials used in this study were three BOF hot rolled steel plates, 25 mm thickness, of JIS SM-50 type, supplied by Nippon Kokan K. K., Kawasaki, Japan (courtesy of Messers. C. Ouchi and J. Tanaka). The chemical analyses are given in Table I. Tensile samples were prepared from the longitudinal (L), transverse (T) and thickness (Z) directions for each of the plates. Two rods (16 mm diameter) were friction-welded before each of the tensile samples in the thickness direction was prepared. The reduced gauge section was 6 mm diameter and 40 mm long for the L and T directions, whereas it was 5 mm diameter and 19 mm long for the Z direction in order to eliminate the influence of the weld zones.

TABLE I Chemical Composition

Steel	Thickness	C	Si	Mn	P	S	Aℓ
		0.17	0.35	1.36	0.015	0.006	0.045
BOF	25 mm	0.15	0.36	1.29	0.021	0.020	0.032
		0.17	0.37	1.42	0.027	0.027	0.037

Mechanical tests were performed with a floor model Instron at room temperature. Nominal strain rate was 5×10^{-4} s^{-1} for the L and T direction and 1×10^{-3} s^{-1} for the Z direction, respectively.

AE tests utilized a wideband sensor fabricated from a PZT-5 element (compressional mode, 3 MHz fundamental frequency, 6.3 mm diameter). It was mounted at the end of a round tensile sample with viscous resin. A preamplifier with a 30 to 2,000 kHz bandpass filter plug-in (Model 160, Acoutic Emission Technology Corp. (AETC), Sacramento, Calif.), a signal processor (Model 201, AETC) and a modified video tape recorder (Sony AV-3650, modified by AETC for AE signal recording) were utilized. The input noise level was 3.2 μV. Amplitude distribution analysis of AE counts was performed by using a specific analyzer (model 203, AETC) or by repeated processing of recorded signals and manual data reduction. Slight variations in the recording level were corrected by the level of background signal. Power density spectrum of a short duration signal (1 to 10 ms long, typically 5 ms) was determined by first obtaining the autocorrelation function using a random signal analyzer (Model 810A, Progress Electronics,

Portland, Oregon) and subsequently taking its Fourier transform via a minicomputer (PDP 8/E, Digital Equipment Corp. together with Analogic Model 5800 analogue-digital-analogue converter). Details of the AE instrumentation have been described elsewhere (5-8).

RESULTS AND DISCUSSION

Observed AE behavior during the tensile tests of the three steel plates in the longitudinal or transverse direction was similar to the well known AE characteristics of a mild steel; i.e., AE activities are significant only during the Lüders band extension or the initial yielding and are very low during the subsequent work-hardening stage. A typical example is shown in Fig. 1. Here, the rms voltage (V_r) vs. time and AE event counts (N_e) vs. time curves of a transverse tensile specimen (no. 6) of the low S steel are shown together with the stress-time curve of the specimen. The corresponding scale for plastic strain is indicated. Note that the stress-time curve is displaced by 13 seconds to the left. During the elastic loading, the level of V_r remained at that of background. At the onset of macroscopic plastic deformation, V_r increased above background and stayed at high levels during the Lüders elongation. In this or other samples in the transverse direction, no upper yield point was displayed in contradistinction to the yield point behavior of samples in the longitudinal direction. Typically, the peak level of V_r was about twice the background. During the work hardening state, V_r was barely above the background. No AE signal was detected during necking. The observed AE activities in samples of the L and T directions were essentially unaffected by the direction or by the variation in the S content.

The waveform of the signal from the longitudinal or transverse samples was always that of the continuous emission. In high S specimens, a small number of short burst signals was also observed. Reflecting the nature of

observed AE signals, AE event counts were quite low in these samples. In Fig. 1, N_e is shown to reach about 2200 for the entire test. Actually, the majority of the observed AE event counts originated from statistically existing peaks of the continuous-type AE signals during the initial yielding*. A valid value of N_e is estimated to be less than 500.

The power density function of the continuous AE signal during the yielding (5.5 ms segment; a low S, transverse sample) is shown in Fig. 2. The frequency spectrum indicates a strong component at 90 kHz, which corresponds to the fundamental resonance of extensional waves in the reduced gauge section (effective length 5.8 cm). A weak component centered at 460 kHz corresponds to radial mode of the transducer, and is only slightly above the background level.

When these steels were tested in the thickness (Z) direction, the yield and tensile strength levels were unchanged from their counterparts in the L and T directions. However, the Lüders and uniform elongations were reduced and the reduction in area was significantly decreased. The AE characteristics of tensile specimens in the thickness direction were also quite different from those described above. Figures 3 and 4 show the V_r vs. time (or strain) curves as well as the corresponding stress-time (or strain) curves of two representative samples in the Z direction. AE activities as exemplified by V_r exhibited two peaks. The first peak coincided with the yielding. AE signals rose above the background at 30% of the yield stress and increased during apparently

---

*In the tests, the reset threshold level of the amplitude distribution analyzer (Model 203, AETC) was set at 16 dB above the background level. Counting of these statistical peaks can be avoided when the reset threshold level is set at 12 dB above the rms voltage of the wideband Gaussian noise.

elastic loading. The level of V_r decreased toward the end of the Lüders elongation, but, with further deformation, V_r reached another maximum at approximately 1.5% plastic strain. The peak level of V_r at the second maximum was lower than that of the first. During work hardening, AE activities persisted, albeit decreasing with increasing strain. The level of V_r was above background up to 8% plastic strain in the low S sample (Fig. 3) and to 13% in the high S sample (Fig. 4). The intensity of AE signals increased with increasing S content. The peak value of V_r in the low S sample was about twice the background, whereas that in the high S sample was almost 5 times the background level.

The N_e vs. time curve is also presented in Fig. 3. Total event counts of this low S sample was 15,400 counts, 95% of which were produced during the initial 5% plastic deformation. While the corresponding curve for N_e is not shown, the high S sample (Fig. 4) produced a total of 65,000 counts. Again, the initial 5% plastic deformation accounted for 95% of the total counts. In the Z direction samples, numerous burst-type signals were found in addition to the continuous AE signals above background noise. These burst signals decayed to the level of continuous signals with 100 to 200 μs. With increases in the S content, the number of burst-type signals increased significantly and the amplitude of the burst-type signals was about twice that observed in the low S specimen. Additionally, a group of three or four burst emission were often found almost consecutively. The frequency spectrum of AE signals containing the burst emission is shown in Fig. 5 (5 ms segment; a high S, Z direction sample). The radial resonance peak at 450 kHz was the highest, and a few satellite peaks were present between 440 and 480 kHz. The extensional wave resonance at 90 kHz was observed, but at a reduced intensity. Other peaks at 150 to 300 kHz also exceeded the background level.

Cumulative AE event amplitude distribution, F_e, was obtained as a function of amplitude for burst emissions. Figure 6 shows a typical result for a medium S, Z direction sample, taken at a plastic strain range of 0.3 to 0.45% during Lüders elongation. Amplitude is given in reference to that at the preamplifier input. A usual power law function yielded a poor fit to the observed distribution, although it may be approximated by a power law having the exponent of unity. The observed distribution function appears to consist of two components; one at low amplitude levels (below 30 μV) due to plastic deformation and the other due to MnS inclusions.

Results of this study indicate the following: (1) Samples in the L and T direction exhibited continuous-type AE primarily during initial yielding, which was unaffected by the S content. Few burst-type AE signals were observed. (2) AE from samples in the Z direction was dominated by burst-type AE and its intensity increased with the S content.

Microstructures of the steels used in this study were usual banded ferrite-pearlite mixtures. Strong dependence on the S content was observed in stringer-type inclusions. Fracture surfaces of the Z direction samples revealed the fracture or decohesion of MnS inclusions flattened during hot rolling. Three mechanisms of AE generation are expected in this material. These are (i) plastic deformation of ferrite matrix, (ii) shearing of pearlite and (iii) the fracture or decohesion of the stringer-type MnS inclusion. The first two, especially pearlite shearing, appear to produce continuous-type AE. This has been supported by a series of experiments using nominally pure iron, AISI Type 1020, 1045, 1080 and W 1 steels. In ferritic-pearlitic conditions, these materials produced continuous-type AE during yielding and its intensity increased with pearlite content. In 1080 and W 1 steels, the interlamellar spacing of pearlite had a strong influence on the intensity of continuous-type AE. Because of an extremely large number of cementite plates within

pearlite, shear cracking of pearlite as originally proposed by Miller and Smith (7) is expected to produce the AE behavior as observed.

Burst-type signals in the Z direction samples can be attributed to the fracture or decohesion of MnS inclusions because of the observed dependencies of AE bursts on the directionality and the sulphur content. It is further supported by the characteristic fracture surface of tensile specimens, and the observed densities of stringer-type inclusions. In order to evaluate stress concentration effects in and around the inclusion, Eshelby theory of transformation strain was employed (8,9). Internal stresses due to misfit strain, inhomogeneity in the elastic moduli and plastic deformation around a non-deformable inclusion were determined (10). It was found that the plastic deformation effect is negligible in the elastic range and that the misfit effect contributes nearly one-third of tensile stress on the broad face, where the magnitude is about 1.5 times that of applied stress. This stress concentration effect at MnS inclusions in the Z direction sample accounts for AE activities at well below the yield stress. Continued AE activities in the work hardening state appear to come from the plastic deformation effect. In contrast, carbide cracks and transverse cracks of pearlite have been found to become observable only after 4 to 10% plastic strain (11). These can be ruled out as sources of burst-type AE found in this study.

In the tensile tests of other steel samples, such as annealed 1020 and normalized 1080 steels, numerous burst-type AE signals were observable even though the tensile direction was longitudinal. For example, a tensile sample of 1020 steel produced a total of 12,300 event counts during the intial 5% plastic strain, as shown in Fig. 7. In the 1020 steel sample, the V_r level was even lower than that shown in Fig. 1. Microscopic examinations

indicated a large number of non-metallic inclusions of various shapes and sizes. The observed burst emissions can be attributed to the fracture or decohesion of these inclusions, although grain boundary carbides may also contribute at later stages of plastic deformation.

CONCLUSIONS

Observed continuous-type AE signals of HSLA steels can be correlated to the plastic deformation of ferrite and pearlite shearing, whereas the burst-type AE signals to the fracture or decohesion of MnS inclusions on the basis of directionality and sulphur dependence. Microscopic examination and elasticity analysis have contributed to the conclusions.

ACKNOWLEDGEMENT

The authors are grateful to Mr. Robert Landy for experimental assistance and to Messers. C. Ouchi and J. Tanaka of Nippon Kokan K. K., Kawasaki, Japan for providing us with the HSLA steel samples used in this study. This work was supported by the Physics Program of the Office of Naval Research.

REFERENCES

(1) Acoustic Emission, ASTM STP 505, Philadelphia, Penn., 1972.

(2) A. S. Tetelman, UCLA-ENG-7249, July 1972.

(3) K. Ono, 2nd Acoustic Emission Symp., Tokyo, Japan, JIPA (1974) IV-1.

(4) Montitoring Structural Integrity by Acoustic Emission, ASTM STP 571, Philadelphia, Penn. (1975).

(5) Y. Krampfner, A. Kawamoto, K. Ono, and A. T. Green, "Acoustic Emission Characteristics of Copper Alloys" NASA CR-134766, April 1975.

(6) K. Ono and H. Ucisik, Mat. Eval. 34 (1976) 32-44.

(7) L. E. Miller and G. C. Smith, J. Iron Steel Inst. 208 (1970) 998.

(8) J. D. Eshelby: Proc. Roy. Soc. A241 (1957) 376.

(9) K. Tanaka and T. Mori, Acta Met. 18 (1970) 931.

(10) M. Shibata and K. Ono, Acta Met. 26 (1978) (in-press).

(11) A. R. Rosenfield, G. T. Hahn and J. D. Embury, Met. Trans. 3 (1972) 2797.

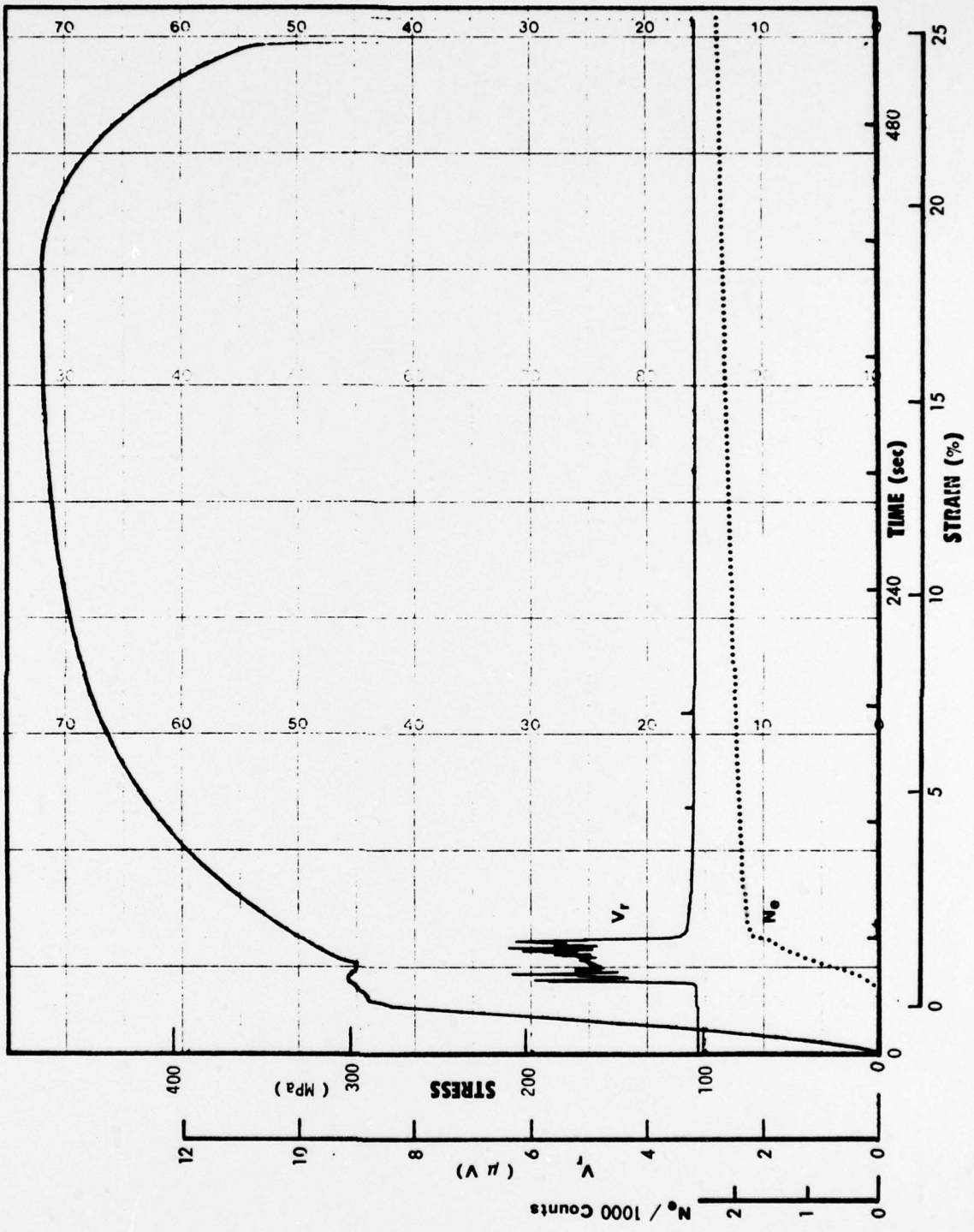

Fig. 1. Stress, V_r and N_e against time or strain for tensile test of a low S, T direction sample.

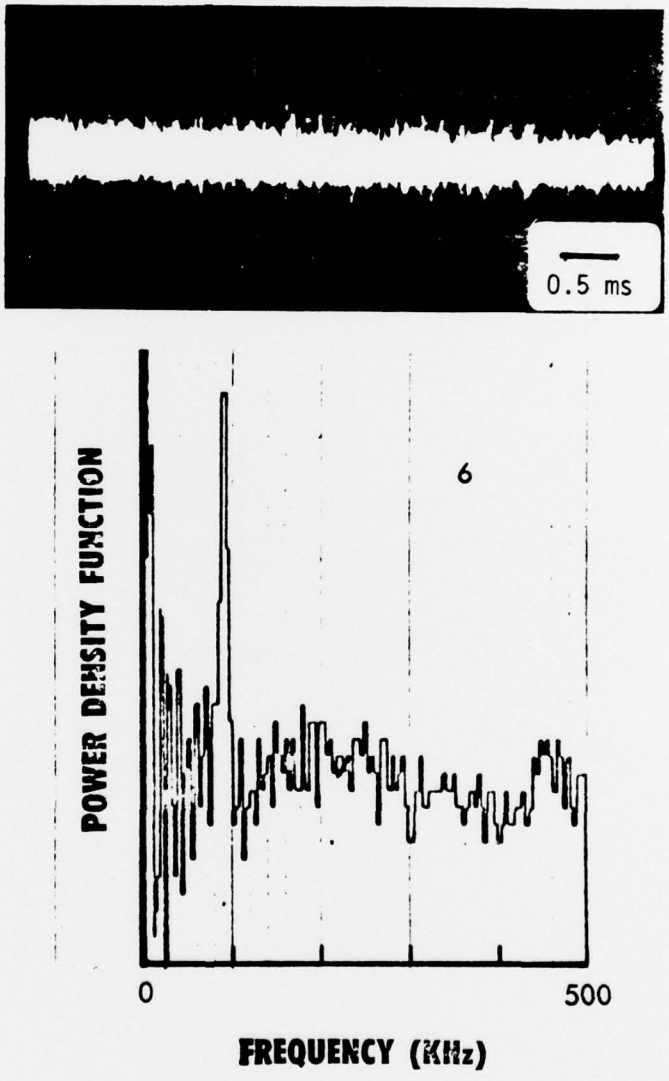

Fig. 2. Waveform and frequency spectrum of continuous-type AE. (Low S; T direction: Specimen No. 6)

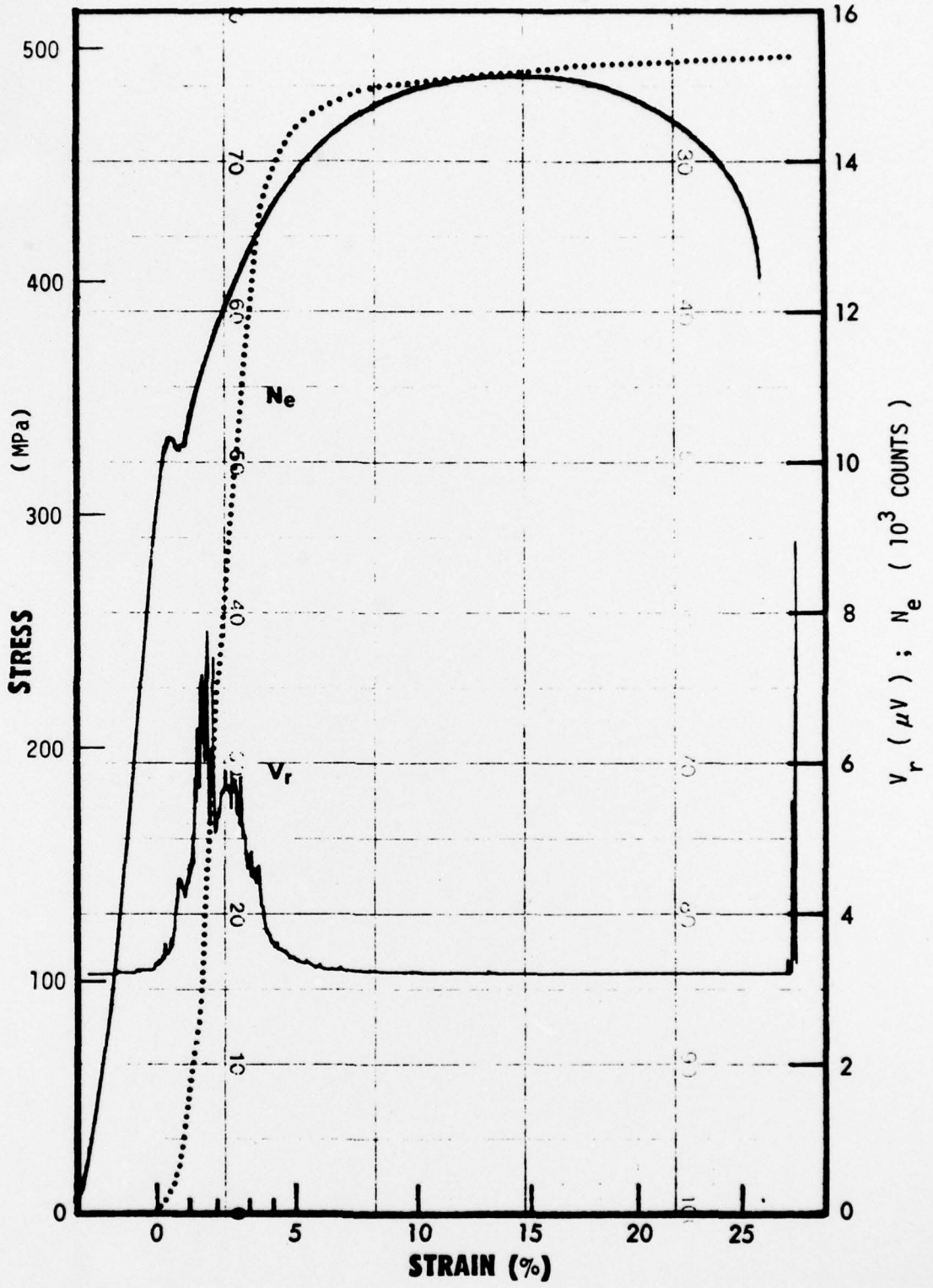

Fig. 3. Stress, V_r and N_e vs. strain (low S; Z direction).

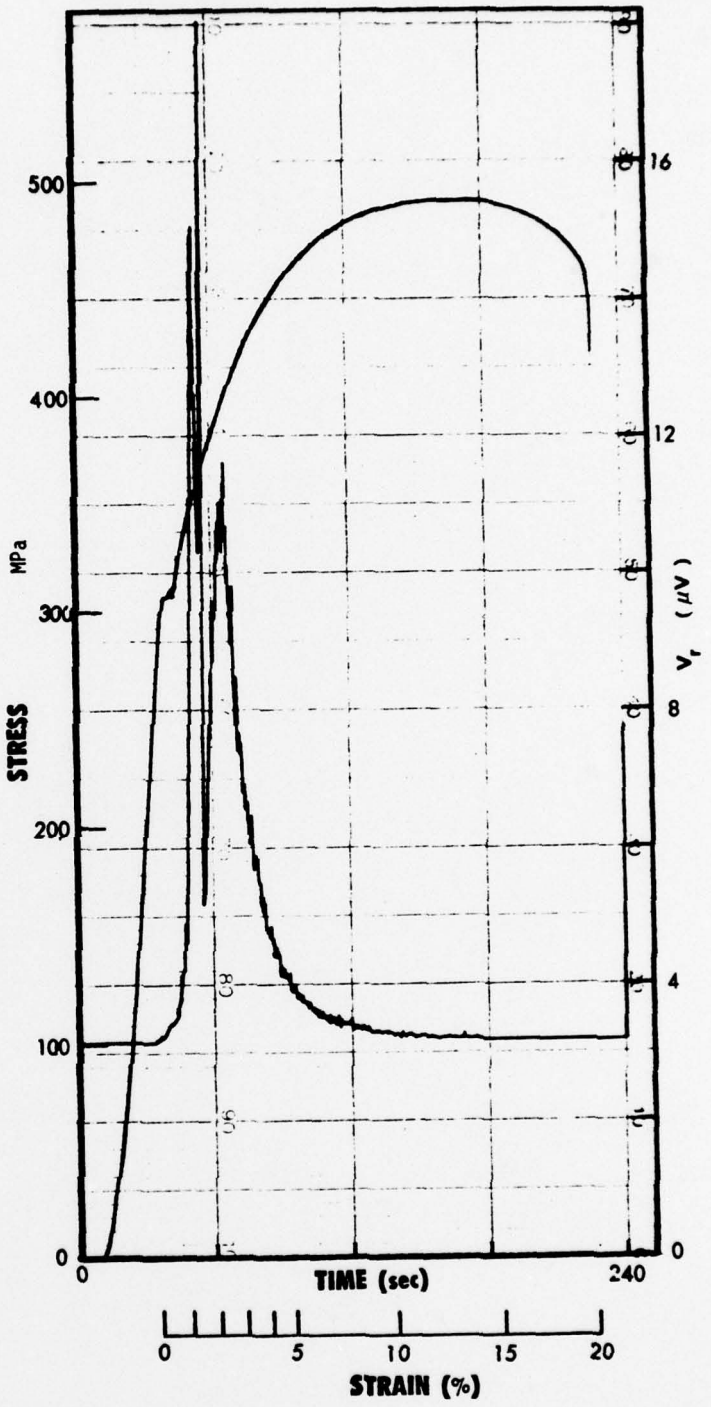

Fig. 4. Stress and V_r vs. time or strain (high S; Z direction).

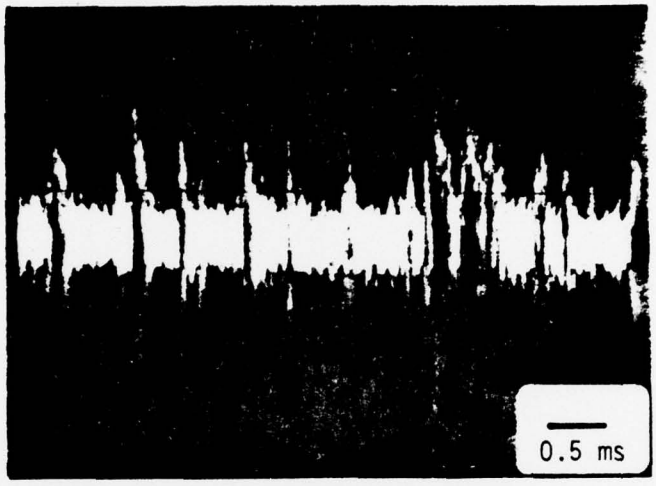

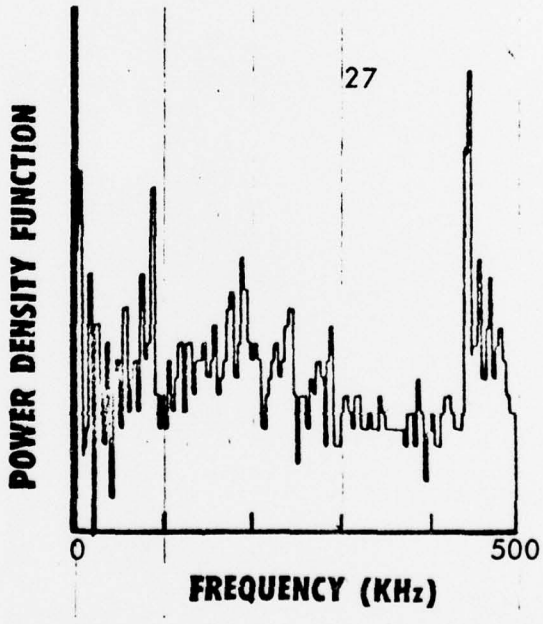

Fig. 5. Waveform and frequency spectrum of burst-type AE. (High S; Z direction: Specimen No. 27).

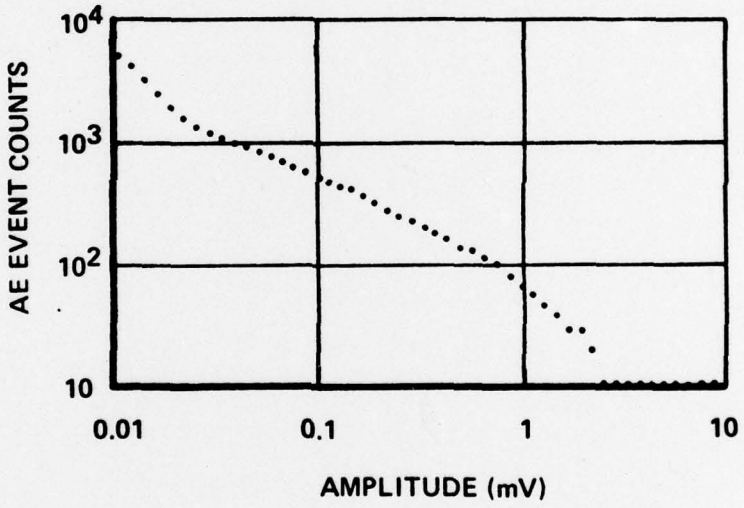

Fig. 6. Cumulative AE event amplitude distribution function against amplitude (medium S; Z direction).

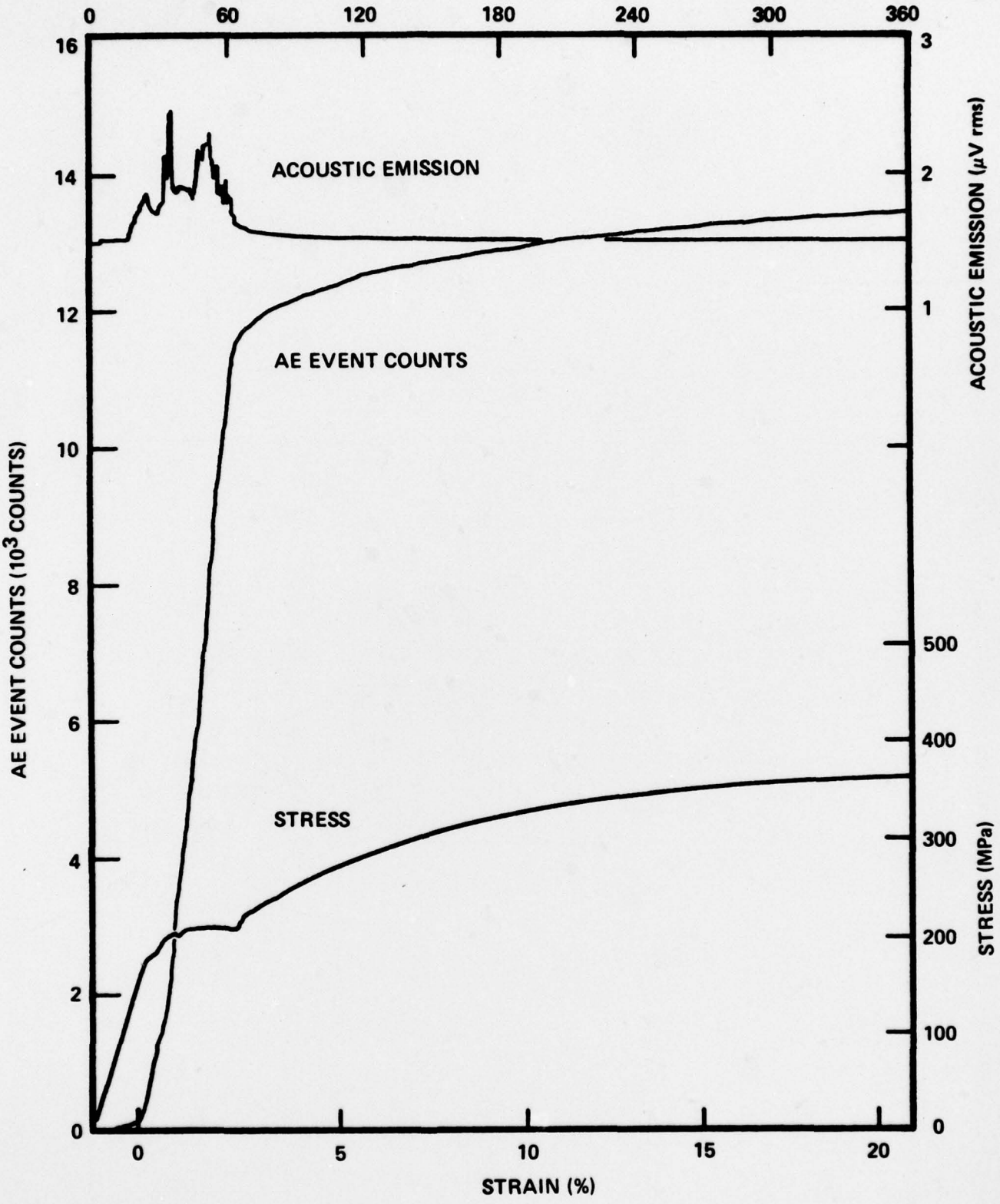

Fig. 7. Stress, AE level and AE event counts against strain or time for tensile test of a 1020 steel sample (annealed at 900°C).